

Nonlocal pair correlations in a higher-order Bose gas soliton

King Lun Ng and Bogdan Opanchuk

Centre for Quantum and Optical Science, Swinburne University of Technology, Melbourne 3122, Australia

Margaret D. Reid and Peter D. Drummond

Centre for Quantum and Optical Science, Swinburne University of Technology, Melbourne 3122, Australia and

Institute of Theoretical Atomic, Molecular and Optical Physics (ITAMP),

Harvard University, Cambridge, Massachusetts, USA.

(Dated:)

The truncated Wigner and positive-P phase-space representations are used to study the dynamics of a one-dimensional Bose gas. This allows calculations of the breathing quantum dynamics of higher-order solitons with $10^3 - 10^5$ particles, as in realistic Bose-Einstein condensation (BEC) experiments. Although classically stable, these decay quantum mechanically. Our calculations show that there are large nonlocal correlations. These also violate the Cauchy-Schwarz inequality, showing the presence of nonclassical quantum entanglement.

A classical soliton [1, 2] is a non-dispersive pulse caused by the balance of dispersion and nonlinearity in a nonlinear wave. Their initial shape can be maintained during propagation. Higher-order classical solitons have additional spatiotemporal oscillations. Time invariant quantum solitons can exist [3, 4], but are completely delocalized in phase and in space. When a coherent soliton is prepared that is classically invariant, quantum effects change the soliton shape. These have been theoretically predicted [5–7] and experimentally verified [8–11].

Higher-order solitons have attracted much recent interest, since their quantum fluctuations can become macroscopically large [12–16]. This leads to a macroscopic quantum initiated decay with fragmentation into multiple condensates, reminiscent of the decay of a false vacuum in scalar quantum field theory [17]. In this Letter, we show that these quantum effects are accompanied by nonlocal dynamical correlations, which occur even before the soliton decays. These fluctuations are largest for a Bose-Einstein condensate soliton formed at mesoscopic particle number. This may be testable in proposed experiments [15] in bosonic ^7Li , with $10^3 - 10^4$ Bose condensed atoms. These correlations survive to very large particle number, and we obtain measurable predictions even for small density changes.

One-dimensional attractive Bose gases form a bright soliton in photonic [18] and Bose-Einstein condensate environments [19–21]. In treatments of these Bose gases, the classical description is known in optics as the nonlinear Schrödinger equation, and in atomic physics as the Gross-Pitaevskii equation [22–24]. This equation uses a mean-field approximation such that operator products are assumed to factorize. In order to include the full quantum properties, beyond mean-field methods are required that include quantum correlations, allowing predictions of rich quantum features. These provide tests of many-body quantum dynamics in a highly controlled, experimentally accessible environment.

An early prediction in photonic systems was the gen-

eration of quantum squeezing and entanglement [5, 6] in one-dimensional bright solitons, verified experimentally in photonic experiments [8, 9, 11]. More recently, there has been interest in the quantum dynamical evolution of higher-order solitons, which oscillate periodically in space at the mean-field level. They can be generated from a fundamental soliton with a *sech* envelope by a rapid increase in the coupling constant. In atomic gases, this is obtainable through a Feshbach resonance. Ultracold atomic physics allows for a strong coupling regime, with fewer particles than in photonics.

Here we use quantum phase space methods to analyze this quench experiment, in which the full many-body quantum state is sampled probabilistically, allowing a calculation of the dynamical evolution of nonlocal correlation functions. These are known to be good indicators of entanglement and possible Bell violations in BEC systems [25–28]. The main technique used is a truncated Wigner (tW) method [29] that employs a $1/N$ expansion for N particles, with $N = 10^3 - 10^5$, as in currently proposed experiments. The general approach has been verified through accurate predictions of quantum squeezing in optical fibre solitons [5, 6, 30]. All the local conservation laws of the bright BEC soliton system are preserved [31]. We also confirm these results using the exact positive-P phase-space representation [32] up to the first oscillation peak.

The density dynamics, but not correlations, have been calculated previously. An approximate variational prediction [13] using the many-body multi-configurational time-dependent Hartree for bosons method (MCTDHB), predicted a sudden fragmentation into two equal fragments. Later work [14], pointed out that this MCTDHB approximation failed to predict the known center-of-mass variance growth. This is because the calculation used only two modes, while there are seven or more condensate modes present [16]. Other methods using exact eigenstates [15] or the DMRG approximation [33], have several orders of magnitude fewer particles.

For Bose gases strongly confined in a one-dimensional waveguide along the r direction with a transverse trapping frequency ω_\perp , the Hamiltonian in the occupation number representation is given by

$$\hat{H}_{1D} = \int dr \left[\frac{-\hbar^2}{2m} \hat{\Psi}^\dagger \frac{\partial^2}{\partial r^2} \hat{\Psi} + \frac{g}{2} \hat{\Psi}^{\dagger 2} \hat{\Psi}^2 \right], \quad (1)$$

where $\hat{\Psi}(r)$ is a one-dimensional quantum field operator.

The total many-body Hamiltonian includes two-body s -wave collisions where $g = 2\hbar a \omega_\perp$ is the interaction strength. This is tunable, since the s -wave scattering length a is a function of the external magnetic field via a Feshbach resonance [34]. Taking a characteristic length scale r_0 and time scale t_0 where $r_0^2 = \hbar t_0 / 2m$, the length and time are transformed into dimensionless form $z = r/r_0$ and $\tau = t/t_0$. The interaction strength g is also transformed into a scaled quantity $C = mgr_0/\hbar^2$. The corresponding Hamiltonian [3, 35] for a system of dimensionless length L is

$$\hat{h} = \int_0^L dz \left[-\hat{\psi}^\dagger(z) \nabla_z^2 \hat{\psi}(z) + C \hat{\psi}^{\dagger 2}(z) \hat{\psi}^2(z) \right]. \quad (2)$$

We assume an initial Poissonian distribution of particle numbers, which is a good approximation to the lowest observed experimental BEC number fluctuations in small condensates of 10^3 particles [36], and corresponds to a coherent state. In the Wigner representation, the field operator $\hat{\psi}(z)$ is replaced by a stochastic field ψ [6, 37, 38], which in a symmetrically ordered mapping is initially

$$\psi(z) = \sqrt{n_0(z)} + \frac{1}{\sqrt{2}} \sum_k \frac{1}{\sqrt{L}} \eta_k e^{ikz}. \quad (3)$$

Here η_k is a complex number with correlations $\langle \eta_k \eta_{k'} \rangle = 0$ and $\langle \eta_k \eta_{k'}^* \rangle = \delta_{kk'}$, while $n_0(z) = \langle \hat{\psi}^\dagger(z) \hat{\psi}(z) \rangle$. An alternative approach is to use the positive-P representation [5, 32], which is exact, equivalent to normal ordering, and has two stochastic fields ψ, ψ^+ with initial values $\psi(z) = \psi^+(z) = \sqrt{n_0(z)}$.

The Bose gas is assumed to be initially trapped with a weakly attractive interaction $C = -2/N$, with $n_0(z) = N \text{sech}^2(z)/2$. At time $\tau = 0$, a rapid change of interaction strength is activated by turning on a negative interaction $C = -8/N$. These parameters are chosen to be the same as that of earlier studies [13, 14, 16]. This is equivalent to an experimental system of photons or atoms with an interaction quench which increases the interaction strength by a factor of 4.

The resulting quantum dynamical equation of motion in the truncated Wigner representation is

$$\frac{d\psi}{d\tau} = i \nabla^2 \psi - 2iC\psi (|\psi|^2 - 2\epsilon) + O(1/N), \quad (4)$$

where $\epsilon = 1/2\Delta z$ is an ordering correction for a computational lattice spacing of Δz . The $O(1/N)$ term represents

higher-order differential operators in the phase-space evolution equations, which are neglected here.

The quantum time-evolution dynamical equations in the positive-P case are [5]:

$$\begin{aligned} \frac{d\psi}{d\tau} &= i \nabla_z^2 \psi - 2iC\psi^+ \psi^2 - i\sqrt{2iC}\psi\eta(\tau, z) \\ \frac{d\psi^+}{d\tau} &= -i \nabla_z^2 \psi + 2iC\psi^{+2}\psi - \sqrt{2iC}\psi^+\eta^+(\tau, z), \end{aligned} \quad (5)$$

with independent complex Gaussian stochastic noises η, η^+ , having non-vanishing correlations:

$$\begin{aligned} \langle \eta(\tau, z) \eta(\tau', z') \rangle &= \langle \eta^+(\tau, z) \eta^+(\tau', z') \rangle \\ &= \delta(\tau - \tau') \delta(z - z'). \end{aligned} \quad (6)$$

The partial differential equations were solved using an interaction picture fourth-order Runge-Kutta (RK4) method, using two different public-domain software packages [39, 40], with identical results in both cases. The results given here use the truncated Wigner method, as it has much lower sampling error for long times in this system. These were replicated up to the first oscillation peak with the positive-P equations, as a check on these results.

A similar calculation has been performed in [16, 31]. This demonstrated that all four local conservation laws are satisfied in the simulations. The time-evolution of the density of the classical soliton system near the center ($z = 0$) oscillates with constant period. However, the true quantum condensate fragments into multiple smaller Bose condensates. Thus, the soliton gradually breaks up due to quantum effects.

Here we investigate the quantum correlations caused by this instability. To do this we compare soliton experiments with different number of particles N while keeping CN constant, so the classical results are the same up to a scaling factor. Defining $n_i = n(z_i) \equiv |\psi(z_i)|^2$, the measurable quantum correlations are given by the second order intensity correlation $G^{(2)}(z_1, z_2) = \langle \hat{\psi}^\dagger(z_1) \hat{\psi}^\dagger(z_2) \hat{\psi}(z_2) \hat{\psi}(z_1) \rangle$ [41]. In terms of the Wigner ensemble averages, this is:

$$G^{(2)}(z_1, z_2) = \langle n_1 n_2 - \epsilon(1 + \delta_{z_1 z_2}) [n_1 + n_2 - \epsilon] \rangle_W. \quad (7)$$

The normalized correlation function is given by

$$g^{(2)}(z_1, z_2) = \frac{\langle \hat{\psi}^\dagger(z_1) \hat{\psi}^\dagger(z_2) \hat{\psi}(z_2) \hat{\psi}(z_1) \rangle}{\langle \hat{n}(z_1) \rangle \langle \hat{n}(z_2) \rangle}, \quad (8)$$

where we note that the product of annihilation and creation operators is expressed in terms of the Wigner representation, so that the expected number density is:

$$\langle \hat{n}(z) \rangle = \langle \hat{\psi}^\dagger(z) \hat{\psi}(z) \rangle = \langle n(z) \rangle_W - \epsilon. \quad (9)$$

The normalized correlation function is used to observe the bunching ($g^{(2)}(z, z) > 1$) and anti-bunching

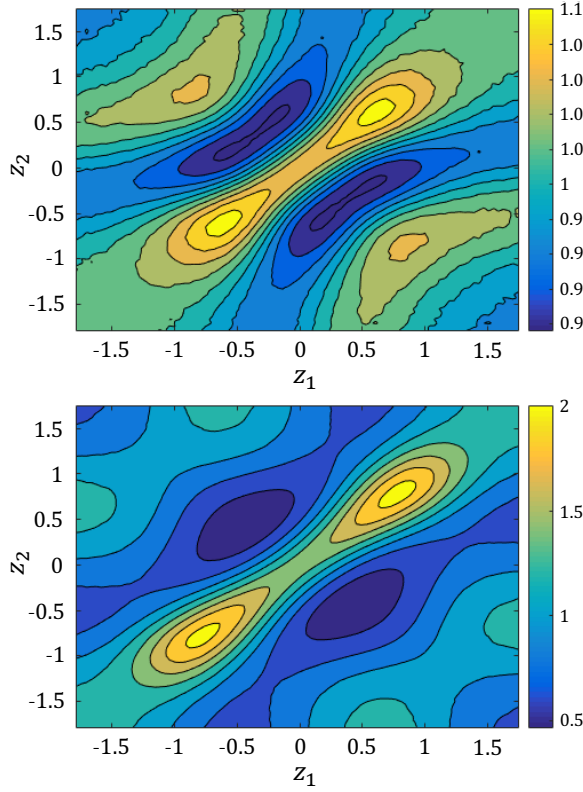


Figure 1. Normalized second order correlation $g^{(2)}(z_1, z_2)$ for $N = 10^3$ at $\tau = 1.0$ (top) and $\tau = 5.0$ (bottom). Here $CN = -8$ and $L = 20$. Simulations have $M = 512$ modes, 9×10^4 trajectories and 9×10^4 time steps. The contour plots show the region within $z = \pm 1.78$. The diagonal axis shows the local correlation $g^{(2)}(\bar{z}, \bar{z})$, with $\bar{z} = (z_1 + z_2)/2$. The anti-diagonal axis shows the nonlocal correlation $g^{(2)}(z_1, z_2)$ where $z_1 = -z_2$. The maximum sampling error is 10^{-2} and the maximum time-step error is 10^{-6} .

($g^{(2)}(z, z) < 1$) amplitude of the soliton. According to the contour plot displayed in Figure 1, for the $N = 10^3$ system, the 1D BEC soliton develops a strong bunching region with peaks of $g^{(2)}$ increasing from ~ 1.1 at $\tau = 1.0$ (Figure 1 top) to ~ 2 at $\tau = 5.0$ (Figure 1).

When using the normally-ordered positive-P representation, the normally ordered averages require no ordering corrections. In this case we define $n_i \equiv \psi^+(z_i)\psi(z_i)$, and one finds that $G^{(2)}(z_1, z_2) = \langle n_1 n_2 \rangle_P$, and $\langle \hat{n}(z) \rangle = \langle n(z) \rangle_P$. This method has no N -dependent truncation, which allows us to confirm that truncation errors are negligible in the Wigner predictions. We find no difference in the results, as expected, given that $N \geq 1000$ for these calculations. Figure 2 shows complete agreement of the two simulations for $g^{(2)}(\Delta z) \equiv g^{(2)}(\Delta z/2, -\Delta z/2)$. This gives nonlocal anti-correlations and correlations at the first peak, occurring at $\tau = \pi/8$.

At larger N values of $N = 10^5$, the peak value of $g^{(2)}$ is significantly reduced to ~ 1.1 at $\tau = 5.0$, which appears to give a weaker bunching within the soliton.

Figures 3 and 4 show the time evolution of the nonlocal correlation, $g^{(2)}(\Delta z/2, -\Delta z/2)$ at different times, for $N = 10^3$ and $N = 10^5$ respectively. These graphs show that the strongest correlations occur near the peak intensities, and are almost unchanged with particle number. What changes with N is the width in time of these correlations, as they remain strong for a much longer time with smaller particle number. The large anti-correlations at long times show that fragmentation occurs to a highly asymmetric output, with a much larger fragment occurring at $+z$ than at $-z$, or vice-versa, leading to strongly negative correlations relative to the vacuum level.

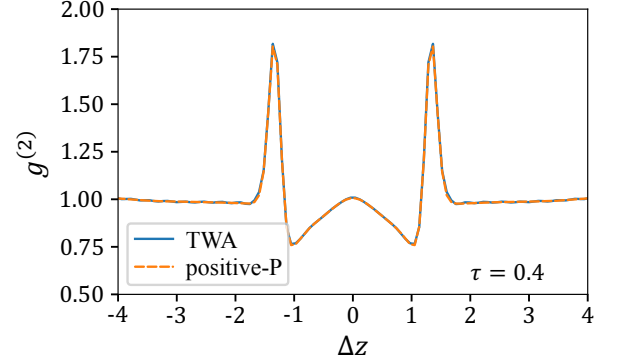


Figure 2. Normalized second order correlation $g^{(2)}(\Delta z) \equiv g^{(2)}(\Delta z/2, -\Delta z/2)$ for $N = 10^3$, $\tau = \pi/8$. Simulations have $M = 512$ modes, 9×10^4 trajectories and 9×10^4 time steps. Graphs compare calculations with the truncated Wigner approximation and exact positive-P representations, showing complete agreement within the width of the graphed lines.

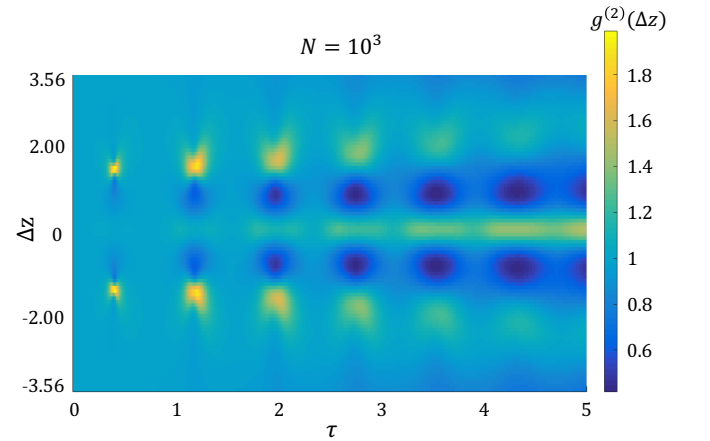


Figure 3. Time-evolution of the normalized second order correlation $g^{(2)}(\Delta z)$, where $N = 10^3$, $CN = -8$ and $L = 20$. Simulations with $M = 512$ modes, 9.6×10^4 trajectories and 9×10^4 time steps. These contours correspond to the correlation along the anti-diagonal axis in Figure 1 which represent the nonlocal correlation. The maximum sampling error is around 0.2% of $g^{(2)}(\Delta z)$.

Next, we ask: are these simply classical correla-

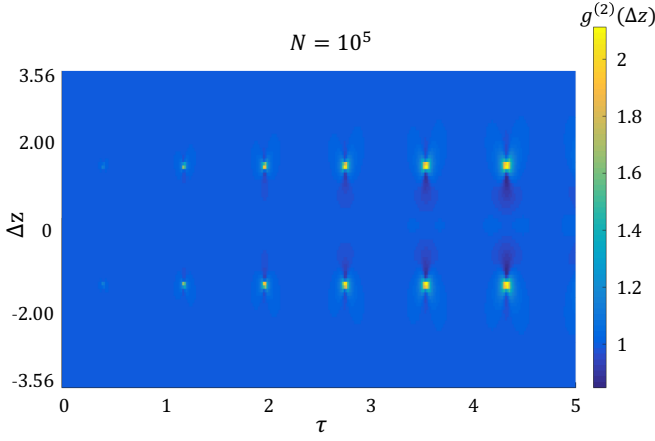


Figure 4. Time-evolution of the normalized second order correlation $g^{(2)}(\Delta z)$, with $N = 10^5$. Other parameters as in Figure 3.

tions, or do they have non-classical, quantum features? Classical correlations obey the Cauchy-Schwarz inequality (CSI), which in terms of the second-order correlation functions, $G^{(2)}(z_1, z_2) = \langle : \hat{n}(z_1)\hat{n}(z_2) : \rangle = \langle \hat{\psi}^\dagger(z_1)\hat{\psi}^\dagger(z_2)\hat{\psi}(z_2)\hat{\psi}(z_1) \rangle$, is given by

$$G^{(2)}(z_1, z_2) \leq \sqrt{G^{(2)}(z_1, z_1)G^{(2)}(z_2, z_2)}.$$

One can introduce a correlation coefficient $C_{CSI} = G^{(2)}(z_1, z_2)/\sqrt{G^{(2)}(z_1, z_1)G^{(2)}(z_2, z_2)}$, to demonstrate that the system possesses nonlocal fluctuations that are stronger than any possible classical fluctuations, when $C_{CSI} > 1$ [25, 28, 41, 42]. For a system of identical bosons, the CSI is violated if the coefficient C_{CSI} is greater than unity. This violation implies that particle entanglement is possible to exist, [43], leading to the potential for tests of Bell correlation via an Ou-Mandel test [44, 45].

For the case of the soliton system with 1000 particles, there is one pair of C_{CSI} -peaks above unity, as shown in Figure 5. The generation of multiple fragmented condensates at later times reduces the strong pairing correlations found at earlier times. The peaks which maximize the CSI correspond to the $g^{(2)}$ -peaks at the same position and the same time ($\Delta z \sim \pm 1.12$, $\tau \sim \pi/8$), as shown in Figure 2 for each N . These low N results have relatively large sampling errors.

Testing the CSI violation with larger numbers of particles N (Figure 6), we find that there are CSI violations at $N > 1000$. However, this reduces as N increases. As already shown in Figures 3 and 4, the normalized non-local correlations $g^{(2)}(\Delta z)$ of the BEC soliton have several peak values. Only the first pair of $g^{(2)}$ -peaks gives a CSI violation. Although the $g^{(2)}$ -peak values remain strong at later time $\tau > \pi/8$ for systems with larger number of particles, no further CSI violations are observed to

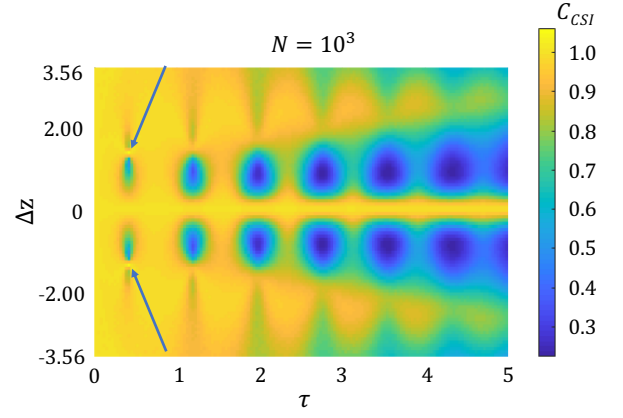


Figure 5. Time-evolution of the correlation coefficient C_{CSI} . $N = 10^3$, $CN = -8$ and $L = 20$ (graph only shows region near the centre $\Delta z = \pm 3.56$). Simulations have $M = 512$ spatial modes, 8×10^4 trajectories and 3×10^4 time steps. The maximum sampling error is around 2%, the time-step error is too small to be seen. Blue arrows indicate the location where CSI is largest.

the accuracy of the present simulations. The soliton fluctuations apparently become more classical as the number of particles in the soliton increases, even though the peak intensity correlations remain very strong.

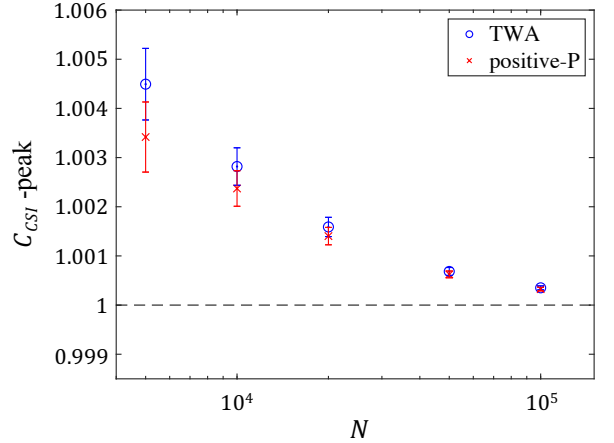


Figure 6. Peak values of correlation coefficient C_{CSI} for Cauchy-Schwarz inequality violations at different particle numbers N . Simulations with 5×10^5 trajectories and 4500 time steps for a time duration $\tau = 0.75$. Errors are dominated by sampling error, which is larger for smaller N . Comparing calculations with the truncated Wigner approximation and exact positive-P representations, showing increasing agreement for higher number of particles.

To summarize, our quantum dynamical calculations predict very strong nonlocal anti-correlations in 1D BEC soliton breathers as they fragment. The oscillatory decay of the nonlocal correlation depends on the particle number N , with the position and the amplitude of the correlation peak being relatively stable at large N , but

with a reduced peak width. There is also a small Cauchy-Schwarz inequality violation, showing that these nonlocal correlations have nonclassical entanglement. This effect is most pronounced at the first peak, and in a system of mesoscopic scale ($N \sim 10^3$). We interpret this as a radiation of entangled, correlated pairs of particles at the soliton peaks, which occurs during soliton fragmentation into asymmetric fragments. At subsequent peaks the strong correlation remains. However, the localized Cauchy-Schwarz inequality violation becomes less pronounced as the quantum many-body system becomes more fragmented during the decay.

PDD and MDR thank the Australian Research Council and the hospitality of the Institute for Atomic and Molecular Physics (ITAMP) at Harvard University, supported by the NSF. PDD acknowledges useful discussions with M. Olshanii. This research has been supported by the Australian Research Council Discovery Project Grants schemes under Grant DP180102470.

-
- [1] J. S. Russell, Report of the 14th Meeting of the British Association for the Advancement of Science (1844).
 - [2] D. J. Korteweg and G. de Vries, The London, Edinburgh, and Dublin Philosophical Magazine and Journal of Science **39**, 422 (1895).
 - [3] J. B. McGuire, J. Math. Phys. **5**, 622 (1964).
 - [4] H. B. Thacker, Rev. Mod. Phys. **53**, 253 (1981).
 - [5] S. J. Carter, P. D. Drummond, M. D. Reid, and R. M. Shelby, Phys. Rev. Lett. **58**, 1841 (1987).
 - [6] P. D. Drummond and A. D. Hardman, Europhysics Letters (EPL) **21**, 279 (1993).
 - [7] H. A. Haus and Y. Lai, JOSA B **7**, 386 (1990).
 - [8] M. Rosenbluh and R. M. Shelby, Phys. Rev. Lett. **66**, 153 (1991).
 - [9] P. D. Drummond, R. M. Shelby, S. R. Friberg, and Y. Yamamoto, Nature **365**, 307 (1993).
 - [10] S. Spälter, N. Korolkova, F. König, A. Sizmann, and G. Leuchs, Physical review letters **81**, 786 (1998).
 - [11] J. F. Corney, J. Heersink, R. Dong, V. Josse, P. D. Drummond, G. Leuchs, and U. L. Andersen, Phys. Rev. A **78**, 023831 (2008).
 - [12] M. J. Werner, Phys. Rev. A **54**, R2567 (1996).
 - [13] A. I. Streltsov, O. E. Alon, and L. S. Cederbaum, Phys. Rev. Lett. **100**, 130401 (2008).
 - [14] J. G. Cosme, C. Weiss, and J. Brand, Phys. Rev. A **94**, 043603 (2016).
 - [15] V. A. Yurovsky, B. A. Malomed, R. G. Hulet, and M. Olshanii, Phys. Rev. Lett. **119**, 220401 (2017).
 - [16] B. Opanchuk and P. D. Drummond, Phys. Rev. A **96**, 053628 (2017).
 - [17] S. Coleman, Phys. Rev. D **15**, 2929 (1977).
 - [18] L. F. Mollenauer, R. H. Stolen, and J. P. Gordon, Phys. Rev. Lett. **45**, 1095 (1980).
 - [19] L. Khaykovich, F. Schreck, G. Ferrari, T. Bourdel, J. Cubizolles, L. D. Carr, Y. Castin, and C. Salomon, Science **296**, 1290 (2002).
 - [20] A. G. T. K. E. Strecker, G. B. Partridge and R. G. Hulet, Nature **417**, 150-153 (2002).
 - [21] J. H. Nguyen, D. Luo, and R. G. Hulet, Science **356**, 422 (2017).
 - [22] E. P. Gross, J. Math. Phys. **4**, 195 (1963), <https://doi.org/10.1063/1.1703944>.
 - [23] E. P. Gross, Il Nuovo Cimento (1955-1965) **20**, 454 (1961).
 - [24] L. Pitaevskii, JETP **13**, 451 (1961).
 - [25] K. V. Kheruntsyan, J.-C. Jaskula, P. Deuar, M. Bonneau, G. B. Partridge, J. Ruauadel, R. Lopes, D. Boiron, and C. I. Westbrook, Physical review letters **108**, 260401 (2012).
 - [26] M. Bonneau, W. J. Munro, K. Nemoto, and J. Schmiedmayer, Physical Review A **98**, 033608 (2018).
 - [27] T. Wasak and J. Chwedeńczuk, Physical review letters **120**, 140406 (2018).
 - [28] M. D. Reid and D. F. Walls, Physical Review A **34**, 1260 (1986).
 - [29] E. P. Wigner, Phys. Rev. **40**, 749 (1932).
 - [30] J. F. Corney, P. D. Drummond, J. Heersink, V. Josse, G. Leuchs, and U. L. Andersen, Phys. Rev. Lett. **97**, 023606 (2006).
 - [31] P. D. Drummond and B. Opanchuk, Phys. Rev. A **96**, 043616 (2017).
 - [32] P. D. Drummond and C. W. Gardiner, J. Phys. A: Math. Gen. **13**, 2353 (1980).
 - [33] C. Weiss and L. D. Carr, arXiv preprint arXiv:1612.05545 (2016).
 - [34] S. E. Pollack, D. Dries, R. G. Hulet, K. M. F. Magalhães, E. A. L. Henn, E. R. F. Ramos, M. A. Caracanhas, and V. S. Bagnato, Phys. Rev. A **81**, 053627 (2010).
 - [35] E. H. Lieb and W. Liniger, Phys. Rev. **130**, 1605 (1963).
 - [36] C.-S. Chuu, F. Schreck, T. P. Meyrath, J. L. Hanssen, G. N. Price, and M. G. Raizen, Phys. Rev. Lett. **95**, 260403 (2005).
 - [37] M. J. Steel, M. K. Olsen, L. I. Plimak, P. D. Drummond, S. Tan, M. J. Collett, D. F. Walls, and R. Graham, Phys. Rev. A **58**, 4824 (1998).
 - [38] B. Opanchuk and P. D. Drummond, J. Math. Phys. **54**, 042107 (2013).
 - [39] S. Kiesewetter, R. Polkinghorne, B. Opanchuk, and P. D. Drummond, SoftwareX **5**, 12 (2016).
 - [40] B. Opanchuk, “Reikna: a pure Python GPGPU library,” <http://reikna.publicfields.net> (2014).
 - [41] R. J. Glauber, Phys. Rev. **130**, 2529 (1963).
 - [42] R. Loudon, Reports on Progress in Physics **43**, 913 (1980).
 - [43] T. Wasak, P. Szańkowski, P. Ziń, M. Trippenbach, and J. Chwedeńczuk, Phys. Rev. A **90**, 033616 (2014).
 - [44] Z. Y. Ou and L. Mandel, Physical Review Letters **61**, 50 (1988).
 - [45] L. Rosales-Zárate, B. Opanchuk, P. D. Drummond, and M. D. Reid, Physical Review A **90**, 022109 (2014).